Alloy theory with atomic resolution for Rashba or topological systems

Zhi Wang,[1] Jun-Wei Luo,[2,3] and Alex Zunger[1,*]

[1]*Renewable and Sustainable Energy Institute, University of Colorado, Boulder, Colorado 80309, USA*

[2]*State Key Laboratory for Superlattices and Microstructures, Institute of Semiconductors, Chinese Academy of Sciences, Beijing 100083, China*

[3]*Beijing Academy of Quantum Information Sciences, Beijing 100193, China*

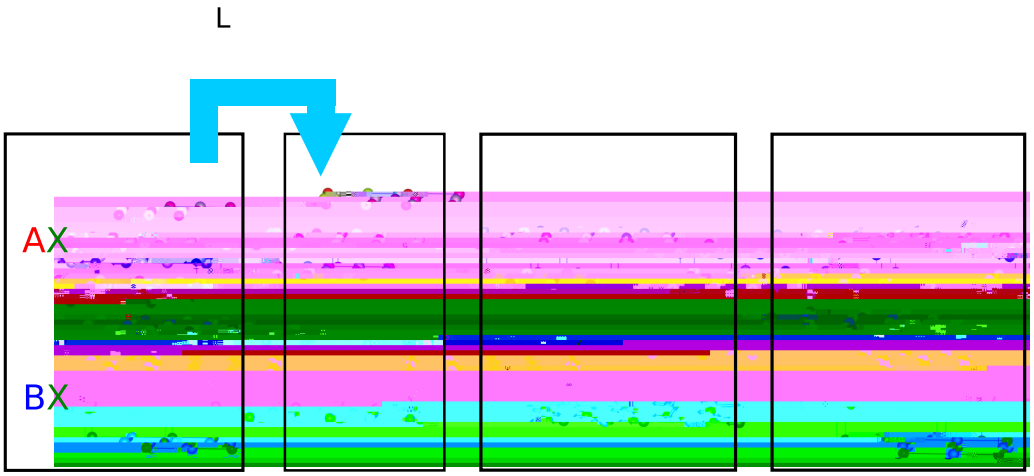
L
AX
BX

TABLE I. The calculation details for pure compounds and the comparison between DFT and experimental results.

Compounds (space group)	Exchange correlation term	Cutoff energy	Lattice constant (DFT)	Lattice constant (Exp.)	Band gap (DFT)	Band gap (Exp.)
CdTe (F–$43m$)	LDA + U (U_{d} = 10 eV)	400 eV	6.410 Å	6.48 Å	0.86 eV	1.65 eV
HgTe (F–$43m$)	LDA + U (U_{d} = 10 eV)	400 eV	6.436 Å	6.46 Å	−0.26 eV	−0.3 eV
PbSe (Fm–$3m$)	GGA + U ($U_{\mathrm{Pb\_s}}$ = 2 eV)	360 eV	6.22 Å	6.12 Å	0.23 eV	0.17 eV
SnSe (Fm–$3m$)	GGA + U ($U_{\mathrm{Pb\_s}}$ = 2 eV)	360 eV	5.99 Å	6.00 Å	0.72 eV	0.62 □ 0.72 eV
PbS (Fm–$3m$)	GGA + U ($U_{\mathrm{Pb\_s}}$ = 2 eV)	360 eV	6.03 Å	5.93 Å	0.3 V	0.29 eV
PbTe (Fm–$3m$)	GGA + U ($U_{\mathrm{Pb\_s}}$ = 2 eV)	360 eV	6.55 Å	6.44 Å	0.2 eV	0.19 eV

formal reaction

$$AX|_{\bar{a}_0(x)} + BX|_{\bar{a}_0(x)} \rightarrow A_{1-x}B_xX|_{\bar{a}_0(x)} \tag{2}$$

representing charge exchange at constant volume and ideal bond geometry.

(3) Bond relaxation (BR) step [from Figs. 1(c) to 1(d)]. Here we take the previous step where a supercell with its attendant charge transfer was already formed and now allow the relaxation for all internal atomic positions at the fixed alloy lattice vectors $\{\bar{a}_0(x)\}$. Note that for each composition the bond lengths are not single-valued but have distributions due to the polymorphous local environment effect, i.e., bond lengths $R^{(n)}_{A-X}(x)$ and $R^{(n)}_{B-X}(x)$ are neighborhood-configuration-dependent [(n)-dependent]. The BR step is a polymorphous effect thus not captured by monomorphous approaches. The change in extensive property $P(x)$ in this step can be modelled by the formal reaction

$$A_{1-x}B_xX|_{\bar{a}_0(x)} \rightarrow \text{relaxed } A_{1-x}B_xX|_{\bar{a}_0(x)}. \tag{3}$$

The total change in extensive property $P(x)$ of alloy relative to the linearly weighted average of the constituents can be written as

$$\begin{aligned}\Delta P_{\mathrm{tot}}(x) &= P(x) - [xP(AX) + (1-x)P(BX)] \\ &= \Delta P_{\mathrm{LD}}(x) + \Delta P_{\mathrm{CE}}(x) + \Delta P_{\mathrm{BR}}(x),\end{aligned} \tag{4}$$

which will assist us in analyzing physical alloy effect.

III. COMPUTATIONAL DETAILS

This work used the computational resources of the Extreme Science and Engineering Discovery Environment (XSEDE) [22

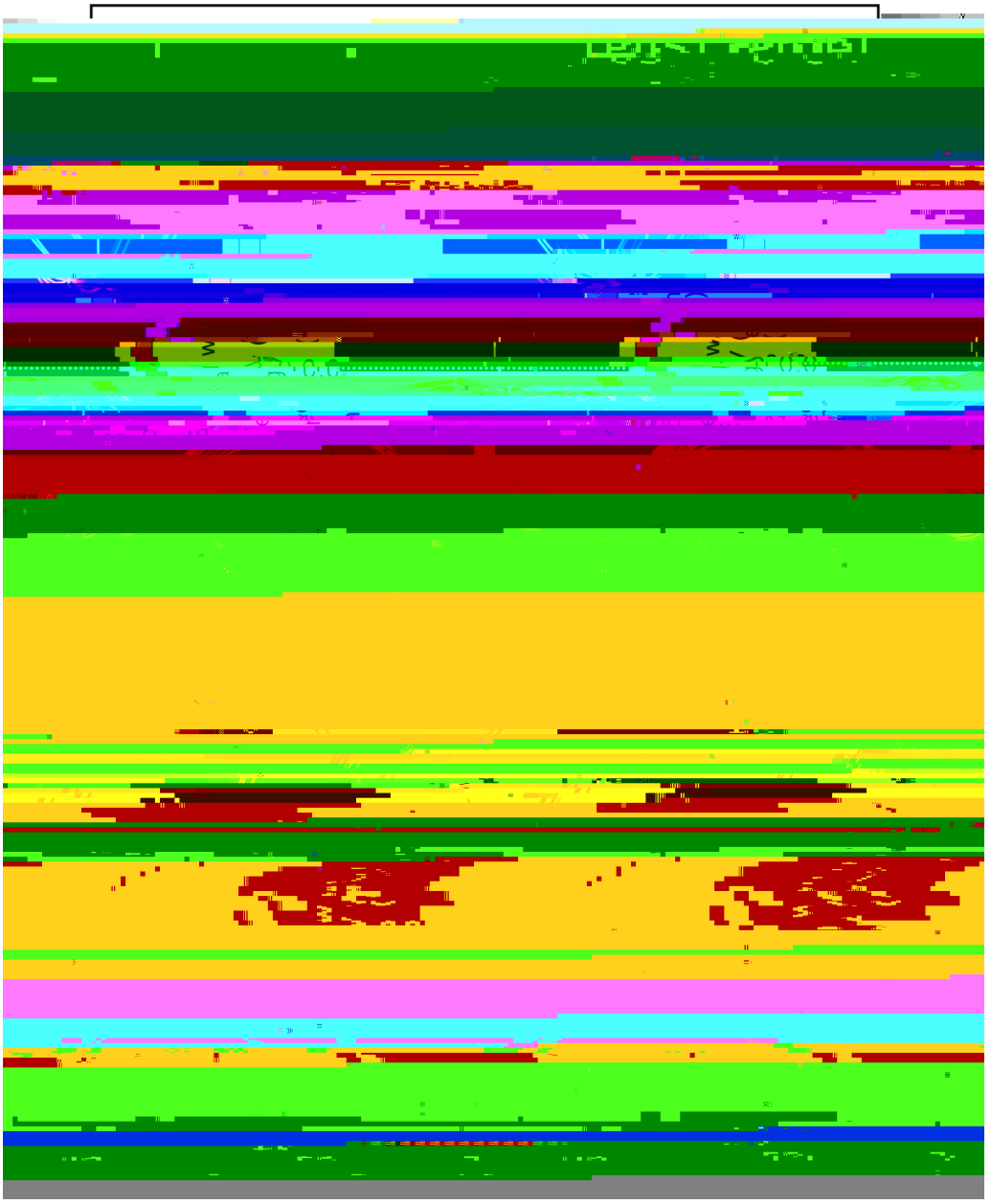

FIG. 7. EBS of PbS-PbTe supercell (32 f.u.) at (a) $S = 9.375\%$, (b) 18.75%, (c) 25%, and (d) 31.25%, unfolded to the distorted *R3m* PbTe primitive Brillouin zone. All EBS are plotted along the same Γ-Z-U direction in the primitive Brillouin zone [$Z = (\pi/a_1,\ \pi/a_2,\ \pi/a_3)$, $U = (\pi/2a_1,\ 2\pi/a_2,\ \pi/2a_3)$]. The white dot lines are only for eye-guiding to show the coherent splitting on VBM along Z-U.

Grants No. 61888102 and No. 61811530022. We thank Qihang Liu for fruitful discussions on the subject. The *ab initio* calculations were done using the Extreme Science and Engineering Discovery Environment (XSEDE), which is supported by National Science Foundation Grant No. ACI-1548562.

APPENDIX: SPECTRAL FUNCTIONS IN ARPES AND IN EBS

When explaining the spectral function of primitive Brillouin zone in ARPES, a common method is to assume the outcoming photoelectron can be described by a single planewave $e^{i\boldsymbol{k}\cdot\boldsymbol{r}}$, i.e., a free-electron final state, therefore the spectral function can be written as [36,37]

$$\tilde{A}(\boldsymbol{k},$$

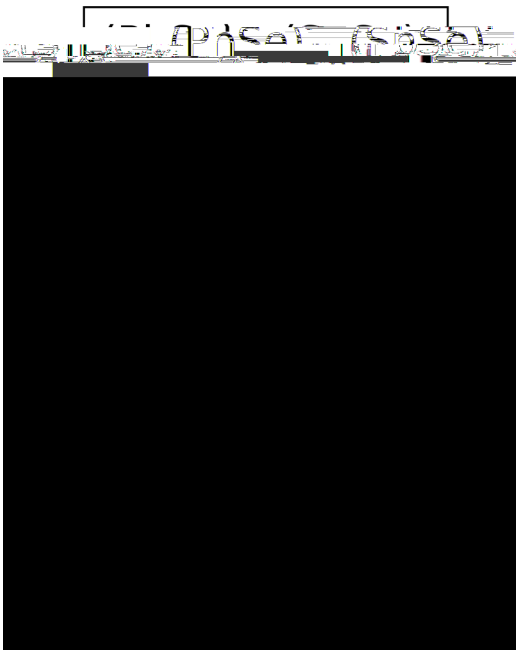

FIG. 8. EBS in a $Pb_{0.75}Sn_{0.25}Se$ 256-atom supercell. $\Gamma = (0,\ 0,\ 0)$, $L_0 = (0.5,\ 0.5,\ 0.5)$, and $\Gamma_2 = (1,\ 1,\ 1)$ (unit of length: $2\pi/a$). The white solid line at L_0 marks the boundary of first and extended BZs. EBS shows the same intensity along path 1 (first BZ) and path 2 (extended BZs).

EBS, meanwhile, offers another way to calculate the spectral function: instead of single planewave, one can use the Bloch function in primitive cell $|\boldsymbol{k}n\rangle$ as the final state, i.e., one calculates spectral function $A(\boldsymbol{k}, E)$ from $|\langle \boldsymbol{k}n | \boldsymbol{K}m\rangle|^2$ instead of $|\langle e^{i\boldsymbol{k}\cdot\boldsymbol{r}} | \boldsymbol{K}m\rangle|^2$ as shown in Eqs. (5)–(7), which is the basic concept of EBS that we describe in Sec. IV. The EBS spectral function $A(\boldsymbol{k}, E)$ from Eq. (7) also represents the $\boldsymbol{k}$ character in $|\boldsymbol{K}m\rangle$, meaning that it is comparable to $\tilde{A}(\boldsymbol{k}, E)$ in Eq. (A1).

Under the single planewave final state assumption [Eq. (A1)], it has been proved that [36] the spectral function $\tilde{A}(\boldsymbol{k}, E)$ can be different at the equivalent $\boldsymbol{k}$ points in different Brillouin zones, e.g., first Brillouin zone and extended Brillouin zone, even when omitting the matrix element effect. However, because the final state is Bloch function, $A(\boldsymbol{k}, E)$ from Eq. (7) has to obey the Bloch theorem, thus $A(\boldsymbol{k}, E)$ is always the same at equivalent $\boldsymbol{k}$ points in different Brillouin zones. As an example, in Fig. 8, we show the EBS of $Pb_{0.75}Sn_{0.25}Se$ 256-atom supercell along the first and extended Brillouin zones: Γ is in first BZ, $L_0 = (0.5,\ 0.5,\ 0.5)$ is on the boundary of first and second BZs, while $\Gamma_2 = (1,\ 1,\ 1)$ (all have unit of $2\pi/a$) is in the extended BZ. The boundaries of first and extended BZs ha boundaries ou6a6i-300.6(ou6a6i-300.6(ou6a6i-

[31] Y. Okada, M. Serbyn, H. Lin, D. Walkup, W. Zhou, C. Dhital, M. Neupane, S. Xu, Y. J. Wang, R. Sankar, F. Chou, A. Bansil, M. Z. Hasan, S. D. Wilson, L. Fu, and V. Madhavan, Science **341**, 1496 (2013).

[32] M. Neupane, S.-Y. Xu, R. Sankar, Q. Gibson, Y. J. Wang, I. Belopolski, N. Alidoust, G. Bian, P. P. Shibayev, D. S. Sanchez, Y. Ohtsubo, A. Taleb-Ibrahimi, S. Basak, W.-F. Tsai, H. Lin, T. Durakiewicz, R. J. Cava, A. Bansil, F. C. Chou, and M. Z. Hasan, Phys. Rev. B **92**, 075131 (2015).

[33] I. Zeljkovic, Y. Okada, M. Serbyn, R. Sankar, D. Walkup, W. Zhou, J. Liu, G. Chang, Y. J. Wang, M. Z. Hasan, F. Chou, H. Lin, A. Bansil, L. Fu, and V. Madhavan, Nat. Mater. **14**, 318 (2015).

[34] T. Phuphachong, B. A. Assaf, V. V. Volobuev, G. Bauer, G. Springholz, L.-A. De Vaulchier, and Y. Guldner, Crystals **7**, 29 (2017).

[35] A. J. Strauss, Phys. Rev. **157**, 608 (1967).

[36] P. Puschnig and D. Lüftner, J. Electron Spectrosc. Relat. Phenom. **200**, 193 (2015).

[37] S. Moser, J. Electron Spectrosc. Relat. Phenom. **214**, 29 (2017).